

Electrochemical Morphine Sensing Using Gold Nanoparticles Modified Carbon Paste Electrode

Nada F. Atta, Ahmed Galal*, Shereen M. Azab

Department of Chemistry, Faculty of Science, Cairo University

Postal Code 12613, Giza, Egypt

*E-mail: galal@sci.cu.edu.eg

Received: 5 August 2011 / Accepted: 2 September 2011 / Published: 1 October 2011

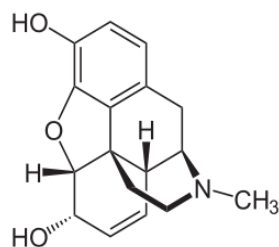
Morphine (MO) is frequently used to relieve severe pain for patients, especially for those who undergo a surgical procedure. However, when overdosed or abused, MO is toxic and can cause disruption in the central nervous system. Therefore, to prevent overdose-induced toxication, it is necessary to sensitively determine the concentrations of MO in patient's blood or urine. An easy-to-use approach for directly electrodepositing gold nanoparticles onto carbon paste electrode (CPE) to construct gold nanoparticles modified carbon paste electrode (GNMCPE) is performed. The electrochemistry of MO is investigated by cyclic voltammetry, differential pulse voltammetry and electrochemical impedance measurements. The data show that this electrode provides a promising approach for highly sensitive morphine sensing that offers an excellent response for morphine in the concentration range of 4.0×10^{-7} to 2.0×10^{-4} mol L⁻¹, with a detection limit of 4.21×10^{-9} mol L⁻¹ and a correlation coefficient of 0.998. GNMCPE has also been successfully applied to the determination of morphine in urine samples with a low detection limit and satisfactory recovery. The good results indicate that GNMCPE holds great promise in practical application

Keywords: Sensor; Carbon paste electrode; Gold nanoparticles; Morphine; Urine samples.

1. INTRODUCTION

Morphine (MO) is a potent opiate analgesic medication and is considered to be the prototypical opioid which can cause disruption in the central nervous system, it is frequently used to relieve severe pain in patients, especially those undergoing a surgical procedure, it works by dulling the pain perception center in the brain. Morphine is a precursor in the manufacture of a large number of opioids such as dihydromorphine, hydromorphone, nicomorphine, and heroin as well as codeine.

Morphine is in a group of drugs called narcotic pain relievers, it is a benzyloquinoline alkaloid with two additional ring closures. (Schematic 1)



Schematic 1.

Morphine is primarily used to treat both acute and chronic pain [1]. It is also used for pain due to myocardial infarction and for labor pains [1]. There are however concerns that morphine may increase mortality in the setting of non ST elevation myocardial infarction [2]. Immediate release of morphine is beneficial in reducing the symptom of shortness of breath due to both cancer and non cancer causes [3, 4].

Morphine interacts predominantly with the μ -opioid receptor. These μ -binding sites are discretely distributed in the human brain, with high densities in the posterior amygdale, hypothalamus, thalamus, nucleus caudatus, putamen, and certain cortical areas. They are also found on the terminal axons of primary afferents within laminae I and II (substantia gelatinosa) of the spinal cord and in the spinal nucleus of the trigeminal nerve [5].

Gold nanoparticles (GNPs) are the subject of intensive research due to their ability to functionalize the surface with self assembled monolayers for many biological based applications, particular large surface area, good bio-compatibility, high conductivity and electrocatalytic activity, so they are used in electrochemical studies [6–10]. GNPs are also suitable for many surface immobilization mechanism and can act as tiny conduction centers and can facilitate the transfer of electrons.

Some analytical methods have been developed for the determination of morphine including high-performance liquid chromatography (HPLC) [11-13]. Fluorescence [14], enzyme-linked immunosorbent assay (ELISA) [15], immunoassay, such as surface plasmon resonance (SPR) based immunosensors [16, 17] and radioimmunoassays (RIA) [18], molecular imprinting technique [19, 20], amperometric methods [21, 22], chemiluminescence [23] and electrochemical methods [24–28] are also reported for morphine detection. Among them, electrochemical methods have also received much interest due to their higher selectivity, lower cost and faster operation than other methods. Bare electrodes as glassy carbon electrode [29] platinum and graphite electrode [30] are used in detection of morphine. Recently, various modified electrodes have been reported for the electrochemical detection of MO as cobalt hexacyanoferrate modified glassy carbon electrode (GCE) [24], Prussian blue-modified indium tin oxide (ITO) electrode [25], molecularly imprinted polymer films to fabricate a microfluidic system for amperometric detection of MO [26], chemically modified-palladized aluminum electrode [31], Au microelectrode [32, 33] in a flow injection system and also multiwalled carbon nanotubes modified preheated glassy carbon electrode has also been used for the morphine detection [34].

The aim of this study is to construct an electrochemical biosensor based on gold nanoparticles and graphite, to be used for the determination of morphine. The electrochemical behaviors of this analgesic compounds at our modified electrode will be investigated using CV and differential pulse voltammetry (DPV) techniques. The detection of MO in tablet and in spiked urine samples without pretreatment will be demonstrated as real sample applications.

2. EXPERIMENTAL

2.1. Materials and reagents

Morphine sulphate was used as received. Britton–Robinson (B–R) (4.0×10^{-2} mol L⁻¹) buffer solution of pH 2–11 (CH₃COOH+H₃BO₃+H₃PO₄), was used as the supporting electrolyte. The pH was adjusted using 0.2 mol L⁻¹ NaOH. All solutions were prepared from analytical grade chemicals and sterilized Milli-Q deionized water.

2.1.1. Construction of gold nanoparticles modified CP-electrode (GNMCPE)

CP-electrode was fabricated as described elsewhere [35] then was immersed into 6 mmol L⁻¹ hydrogen-tetrachloroaurate HAuCl₄ solution containing 0.1 mol L⁻¹ KNO₃ (prepared in doubly distilled water, and deaerated by bubbling with nitrogen). A constant potential of -0.4 V versus Ag/AgCl was applied for 400 s [36]. Then, the modified electrode (GNMCPE) was washed with doubly distilled water and dried carefully.

2.2. Instrumental and experimental set-up

2.2.1. Electrochemical measurements

All voltammetric measurements were performed using a pc-controlled AEW2 electrochemistry work station and data were analyzed with EC_{prog3} electrochemistry software, manufactured by SYCOPEL SCIENTIFIC LIMITED (Tyne & Wear, UK). The one compartment cell with the three electrodes was connected to the electrochemical workstation through a C₃-stand from BAS (USA). A platinum wire from BAS (USA) was employed as auxiliary electrode. All the cell potentials were measured with respect to Ag/AgCl (3 mol L⁻¹ NaCl) reference electrode from BAS (USA). One compartment glass cell (15 ml) fitted with gas bubbler was used for electrochemical measurements. Solutions were degassed using pure nitrogen prior and throughout the electrochemical measurements. A JENWAY 3510 pH meter (England) with glass combination electrode was used for pH measurements. Scanning electron microscopy (SEM) measurements were carried out using a JSM-6700F scanning electron microscope (Japan Electro Company). All the electrochemical experiments were performed at an ambient temperature of 25±0.2°C.

2.2.2. Impedance spectroscopy measurements

Electrochemical impedance spectroscopy was performed using a Gamry-750 system and a lock-in-amplifier that are connected to a personal computer. The data analysis software was provided with the instrument and applied non-linear least square fitting with Levenberg-Marquardt algorithm. The parameters in electrochemical impedance experiment were as follows: different potential values 0.35 V, 0.55 V, were studied at frequency range of 0.1–100000 Hz with amplitude of 5 mV were applied on CPE and GNMCPPE and tested in MO 1.0 mmol L^{-1} .

2.3. Analysis of urine

Standard MO provided by the National Organization for Drug Control and Research of Egypt was dissolved in urine to make a stock solution with $1.0 \times 10^{-3} \text{ mol L}^{-1}$ concentration. Successive additions of MO $1.0 \times 10^{-3} \text{ mol L}^{-1}$ in urine were added to 5 ml B-R buffer pH 7.4.

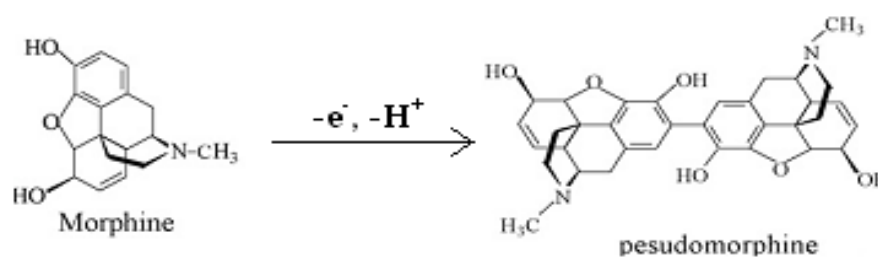
3. RESULTS AND DISCUSSION

3.1. Morphologies of the different electrodes

The response of an electrochemical sensor is related to its physical morphology [9]. The SEM of CP-electrode and GNMCPPE are given elsewhere [9]. Significant differences in the surface structure of CP-electrode and GNMCPPE are observed. The surface of the CP-electrode is predominated by isolated and irregularly shaped graphite flakes and separated layers are noticed. The SEM image of GNMCPPE shows that metallic nanoparticles are located at different elevations over the substrate. Moreover, a random distribution and interstices among the nanoparticles were observed in SEM image of the GNMCPPE exhibiting large surface area.

3.2. Electrochemistry of MO at GNMCPPE

The voltammetric behavior of MO was examined using cyclic voltammetry.



Schematic 2.

Fig 1 shows typical cyclic voltammograms of 1.0×10^{-3} mol L⁻¹ of morphine (MO) in B-R buffer pH 2 (A) and 7.4 (B), at scan rate 100 mVs⁻¹ recorded at two different working electrodes (i.e. a bare CP (solid line) and GNMCPPE (dashed lines) electrodes, respectively). An anodic peak current at +0.722 V in B-R buffer pH 2 and at 0.531 V in B-R buffer pH 7 were produced due to the oxidation of the tertiary amine group of morphine, which produced pseudomorphine as the main oxidative product [36] (Schematic 2).

As can be seen at GNMCPPE the oxidation peak currents in both buffers were higher compared to that of bare CP-electrode, i.e. in case of pH 2 it increases from 40.82 μ A to 102.51 μ A and in case of pH 7 it increases from 29.21 μ A to 54.11 μ A whereas the potential shifted negatively to less positive potentials too, due to the enhancement of the electron transfer process and a larger intrinsic surface area of the modified electrode. The electrodeposition of Au particles on CP-electrode resulted in an observable increase in the peak current, which indicated an improvement in the electrode kinetics and a decrease in the potential of oxidation substantially (i.e. thermodynamically feasible reaction). The results confirmed the key role played by Au nanoparticles on the catalytic oxidation which enhance the electrochemical reaction.

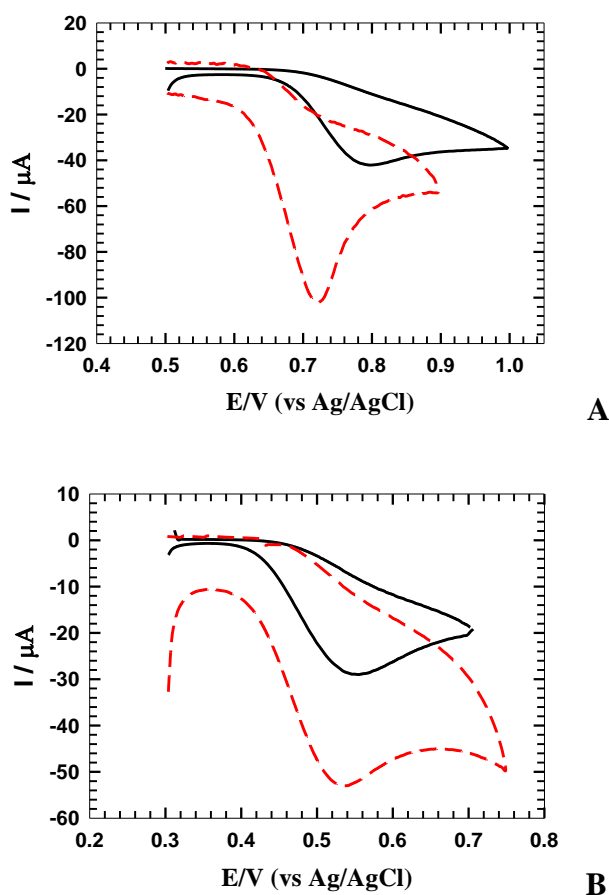


Figure 1. A) Cyclic voltammograms of 1.0×10^{-3} mol L⁻¹ MO in B-R buffer pH 2 at scan rate 100 mVs⁻¹ recorded at two different working electrodes 1) bare CPE (—) and 2) GNMCPPE (----). B) Cyclic voltammograms of 1.0×10^{-3} mol L⁻¹ MO in B-R buffer pH 7.4 at scan rate 100 mVs⁻¹ recorded at two different working electrodes 1) bare CPE (—) and 2) GNMCPPE (----).

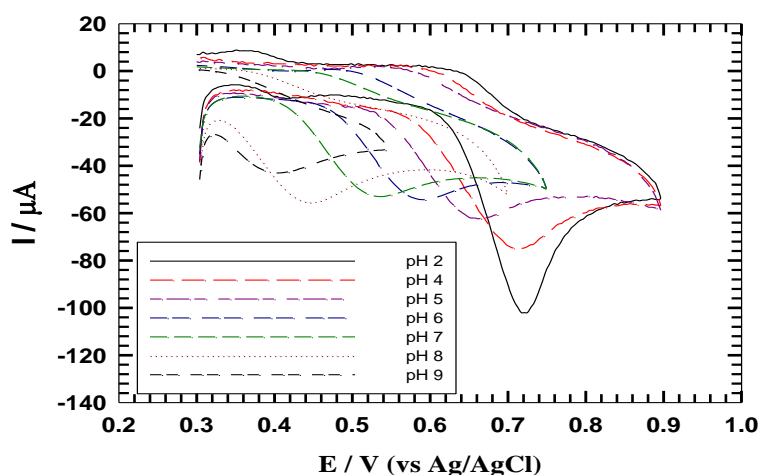
3.3. Effect of operational parameters

3.3.1. Effect of solution pH

Fig. 2A shows the cyclic voltammograms of the oxidation of MO at different pH ranges (2 → 9) using Britton–Robinson buffer. The peak current values were obtained by subtracting the background current density of the GNMCPPE obtained in the pure supporting electrolyte solution from the anodic peak current density obtained for MO oxidation.

A comparison between the anodic peak potential at different pH values of bare CPE and GNMCPPE (fig 2B) shows that the pH of the solution has a significant influence on the peak potential of the catalytic oxidation of MO, i.e. the anodic peak potentials shifted negatively with the increase of the solution pH, indicating that the electrocatalytic oxidation at the GNMCPPE is a pH-dependent reaction and that protons have taken part in their electrode reaction processes. Also, the peak potential for MO oxidation varies linearly with pH (over the pH range from 2 to 11). The relationship between the anodic peak potential and the solution pH value (over the pH range from 2 to 11) could be fit to the linear regression equation of $E_{pa} \text{ (V)} = 0.875 - 0.0538 \text{ pH}$, with a correlation coefficient of $r = 0.967$. The slope was found to be -53.8 mV/pH units over the pH range from 2 to 9, which is close to the theoretical value of -59 mV . This indicated that the number of protons and transferred electrons involved in the oxidation mechanism is equal [37]. As the MO oxidation is one-electron process, the number of protons involved was also predicted to be one indicating an e^-/H^+ process. Although the highest oxidation peak current was obtained at pH 2, other factors will be studied at pH 7.4 (i.e. pH medium of the human body).

Also the comparison between the anodic peak current at different pH values of bare CPE and GNMCPPE (fig 2C) shows that by using GNMCPPE, the oxidation of MO displays higher anodic current responses at low pH values (less than pH 5) than that of bare CPE, while at higher pH values (more than pH 5) the responses are lower, so there is difference in responses at most pH values. This is attributed to the pKa value of morphine ca. 8.08 [38], therefore, the positive charge on MO can be attracted by the negative charge of gold nanoparticles, which indicates the effect of gold nanoparticles on the catalytic oxidation processes.

**A**

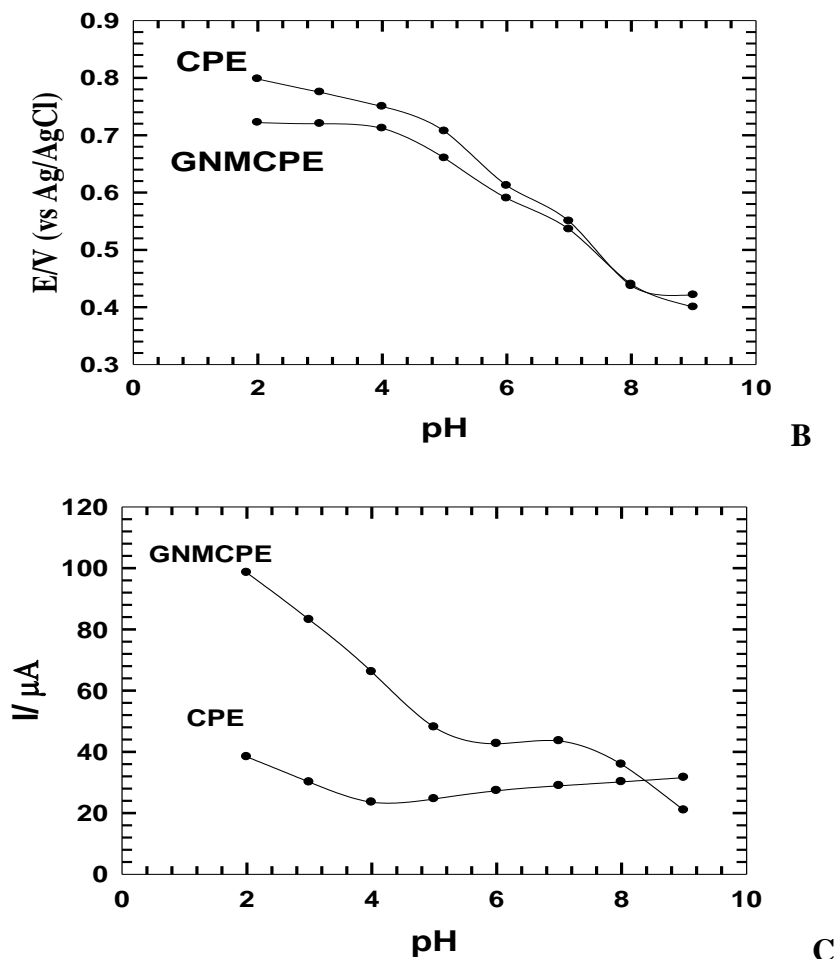


Figure 2. A) Cyclic voltammogram of the effect of solution pH on the electrocatalytic oxidation of MO at GNMCP using Britton–Robinson buffers within the pH range of 2–9. B) Comparison between the anodic peak potentials at different pH values of 1) bare CPE and 2) GNMCP. C) Comparison between the anodic peak currents at different pH values of 1) bare CPE and 2) GNMCE.

3.3.2. Effect of the scan rate

The effect of different scan rates (v ranging from 10 to 250 mVs^{-1}) on the oxidation current response of MO ($1.0 \times 10^{-3} \text{ mol L}^{-1}$) at GNMCP in B-R buffer (pH 7.4) was studied and a plot of i_{pa} versus $v^{1/2}$ gives a straight line relationship. The linearity of the relationship is realized up to a scan rate of 250 mVs^{-1} . This indicates that the charge transfer is under diffusion control. Typical CV curves of MO at different scan rates are shown in Fig 3. The peak potential also increases with the scan rate. A linear relationship is found for the oxidation peak currents and oxidation potentials at different scan rates (Fig 3 inset). The oxidation peak currents increases linearly with the linear regression equations as $i_{\text{pa}} (10^{-6} \text{ A}) = -1.927 v^{1/2} (\text{V s}^{-1})^{1/2} - 4.736$ ($n=7$, $\gamma = 0.9967$), suggesting that the reaction is a diffusion-controlled electrode reaction.

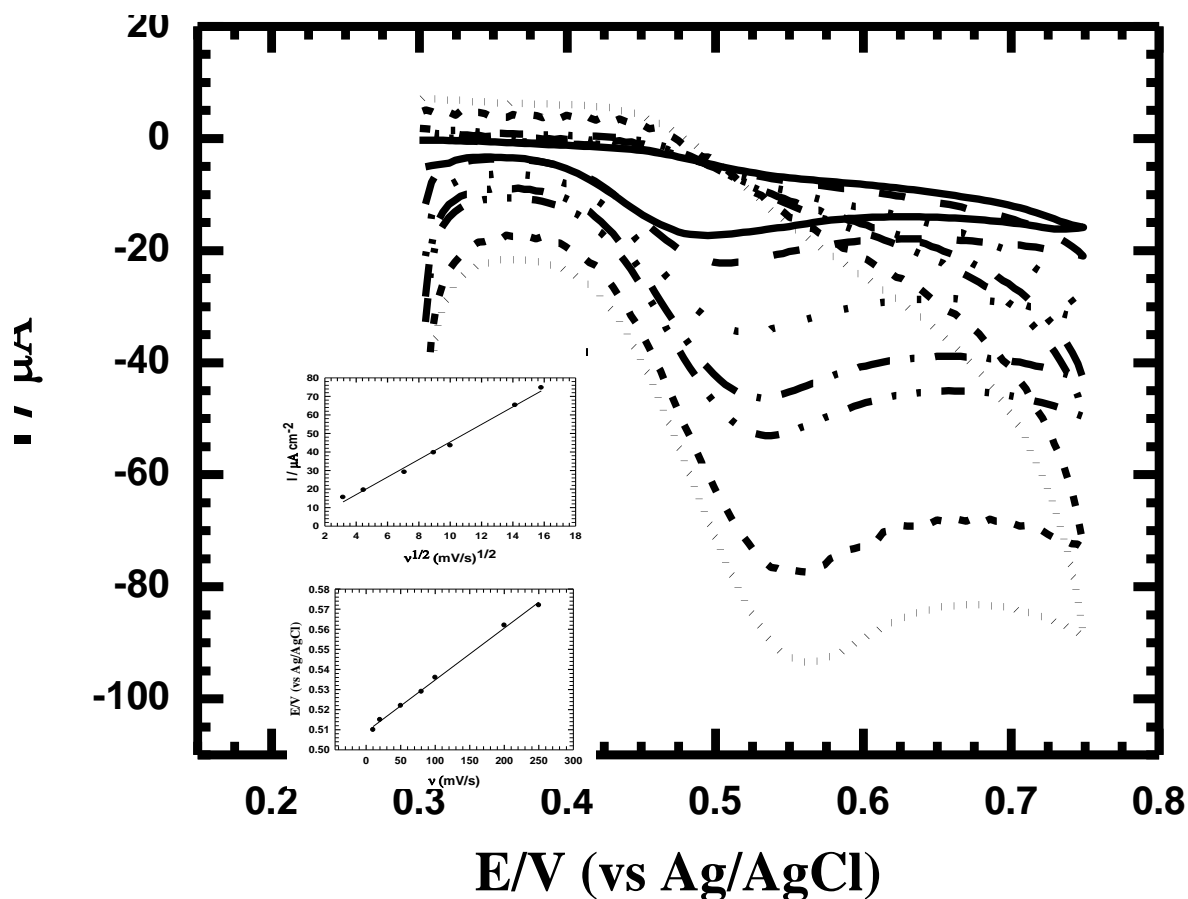


Figure 3. Cyclic voltammograms of $1.0 \times 10^{-3} \text{ mol L}^{-1}$ MO at GNMCPPE in 0.04 M B-R buffer pH 7.4 at: 10, 25, 50, 80, 100, 200 and 250 mV s^{-1} . Inset (1): plot of the anodic peak current values versus square root of scan rate. Inset (2): plot of the anodic peak potential values versus scan rate.

3.3.3. Diffusion coefficients of MO

The dependence of the anodic peak current density on the scan rate has been used for the estimation of the “apparent” diffusion coefficient, D_{app} , for the compounds studied. D_{app} values are calculated from Randles Sevcik equation [39]

$$i_{pa} = (2.69 \times 10^5) n^{3/2} A C_0^* D_0^{1/2} v^{1/2}$$

Where the constant has units $(2.687 \times 10^5 \text{ C mol}^{-1} \text{ V}^{-1/2})$.

In these equations: i_p is the peak current density (mA cm^{-2}), n is the number of electrons appearing in half-reaction for the redox couple, v is the rate at which the potential is swept (V s^{-1}), F is Faraday’s constant (96485 C mol^{-1}), C_0 is the analyte concentration ($1 \times 10^{-6} \text{ mol cm}^{-3}$), A is the electrode area (0.0706 cm^2), and D is the electroactive species diffusion coefficient ($\text{cm}^2 \text{ s}^{-1}$). Apparent surface area used in the calculations did not take into account the surface roughness.

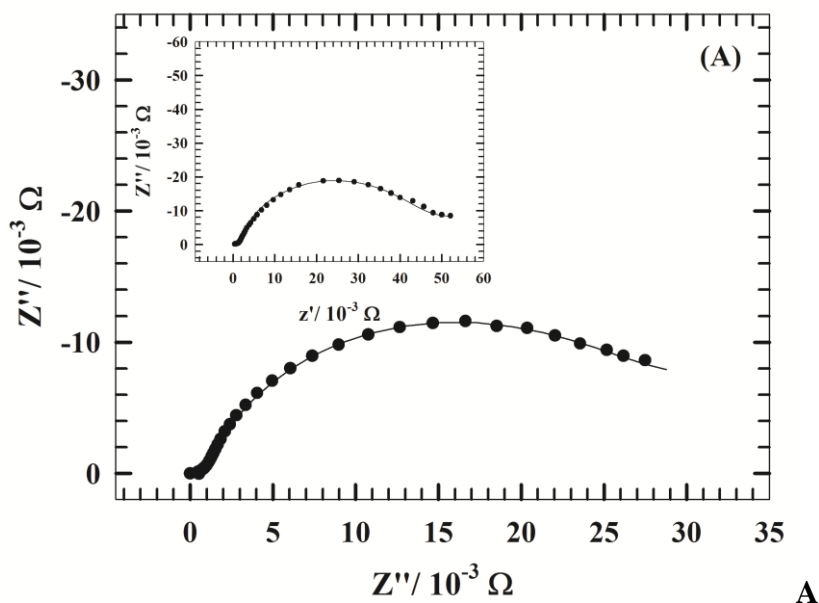
The apparent diffusion coefficients, D_{app} , of MO on GNMCPPE in B-R buffer (pH 7.4) were calculated from cyclic voltammetry (CV) experiments and is found to be $6.57 \times 10^{-6} \text{ cm}^2 \text{ s}^{-1}$. This result is compared to that in case of bare CP-electrode which is $2.71 \times 10^{-6} \text{ cm}^2 \text{ s}^{-1}$. This indicated the quick mass transfer of the analyte molecules towards GNMCPPE surface from bulk solutions and/or fast electron transfer process of electrochemical oxidation of the analyte molecule at the electrode-solution interface [40,41].

Furthermore, it also shows that the redox reaction of the analyte species took place at the surface of the electrode under the control of the diffusion of the molecules from solution to the electrode surface. The calculated D_{app} values at bare CP-electrode and GNMCPPE showed that Au nanoparticles improves the electron transfer kinetics at the electrode/solution interface.

3.4. Electrochemical impedance spectroscopy (EIS) studies

EIS is an effective tool for studying the interface properties of surface-modified electrodes. EIS data were obtained for GNMCPPE at ac frequency varying between 0.1Hz and 100 kHz with an applied potential in the region corresponding to the electrolytic oxidation of MO in B-R buffer pH 7.4. Figure 4 show a typical impedance spectrum presented in the form of Nyquist plot of MO using GNMCPPE at different oxidation potentials: 550 mV (A) and 350 mV (B) and compared to that of the bare CP-electrode (the insets, respectively). From this comparison, it is clear that the impedance responses of MO show great difference in the presence of gold nanoparticles.

The semicircle diameter in the impedance spectrum equals the electron-transfer resistance, R_{et} . This resistance controls the electron-transfer kinetics of the redox probe at the electrode interface.



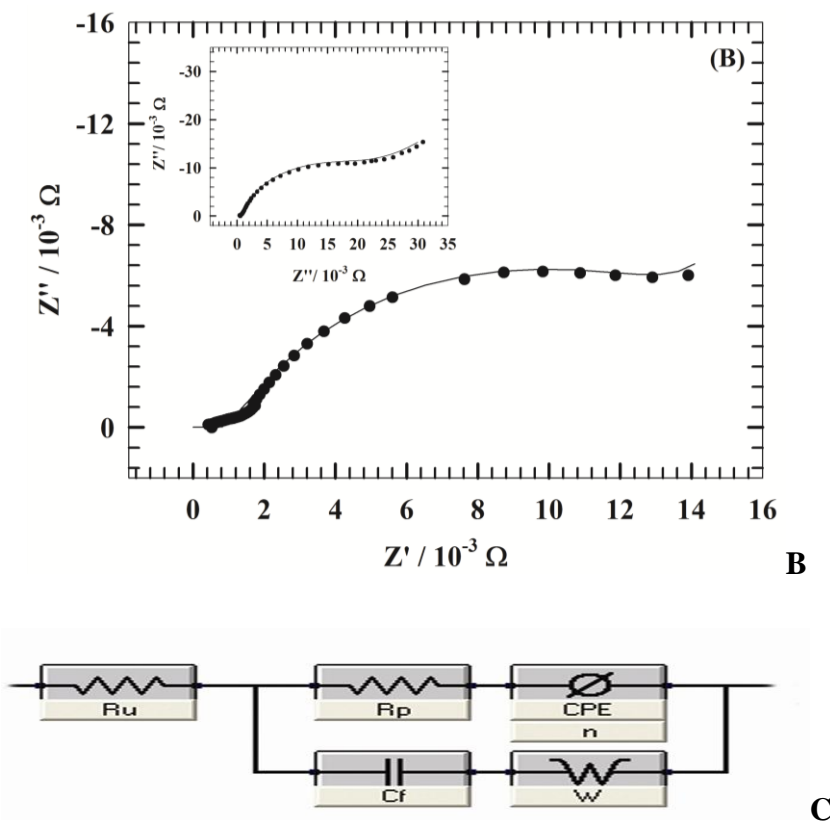


Figure 4. **A)** The typical impedance spectrum presented in the form of Nyquist plot of MO using GNMCPe at the oxidation potential 550 mV. Inset: The typical impedance spectrum presented in the form of Nyquist plot of MO using bare CPE at the oxidation potential 550 mV. (Symbols and solid lines represent the experimental measurements and the computer fitting of impedance spectra, respectively). **B)** The typical impedance spectrum presented in the form of Nyquist plot of MO using GNMCPe at potential 350 mV. Inset: The typical impedance spectrum presented in the form of Nyquist plot of MO using bare CPE at potential 350 mV. (Symbols and solid lines represent the experimental measurements and the computer fitting of impedance spectra, respectively). **C)** Equivalent circuit used in the fit procedure of the impedance spectra.

Table 1. Electrochemical impedance spectroscopy fitting data corresponding to Fig 4A & 4B

Electrode	E/mV	R_p ($k\Omega \text{ cm}^2$)	R_u ($k\Omega \text{ cm}^2$)	C_f (μFcm^{-2})	W ($k\Omega^{-1}\text{cm}^{-2}$)	CPE (μFcm^{-2})	n
Bare CP Electrode	350	22.22	0.41	1.13	40.07	11.50	0.34
	550	20.92	0.46	3.41	35.10	14.41	0.49
GNMCPe	350	21.60	0.44	10.07	32.00	22.20	0.79
	550	15.00	0.40	12.31	30.02	25.34	0.7

Therefore, R_{et} can be used to describe the interface properties of the electrode. To obtain the detailed information of the impedance spectroscopy, a simple equivalent circuit model in Fig 4C was used to fit the results.

In this circuit, R_u is the solution resistance, R_p is the polarization resistance, CPE represents the predominant diffusion influence on the charge transfer process, n is its corresponding exponents, C_f is the capacitance of the double layer and W is the Warburg impedance due to diffusion. Table 1 lists the best fitting values calculated from the equivalent circuit for the impedance data. From the data indicated in Table 1, the value of solution resistance, R_u , is almost constant within the limits of the experimental errors. On the other hand, the ionic/electronic charge transfer resistance shows noticeable decrease in values in case of GNMCPe to CP-electrode which indicates less electronic resistance and more facilitation of charge transfer.

The capacitive component of the charge at the GNMCPe is relatively higher compared to that at CP-electrode. This is explained in terms of the increase in the ionic adsorption at the electrode/electrolyte interface. Moreover, the decrease in the interfacial electron transfer resistance is attributed to the selective interaction between gold nanoparticles and MO that resulted in the observed increase in the current signal for the electro-oxidation process.

3.5. General procedure for the determination of MO in the pure form

The three electrodes are immersed in 5mL of B-R buffer solution of pH 7.4. Since dissolved oxygen does not interfere with the anodic voltammetry, no deaeration was performed.

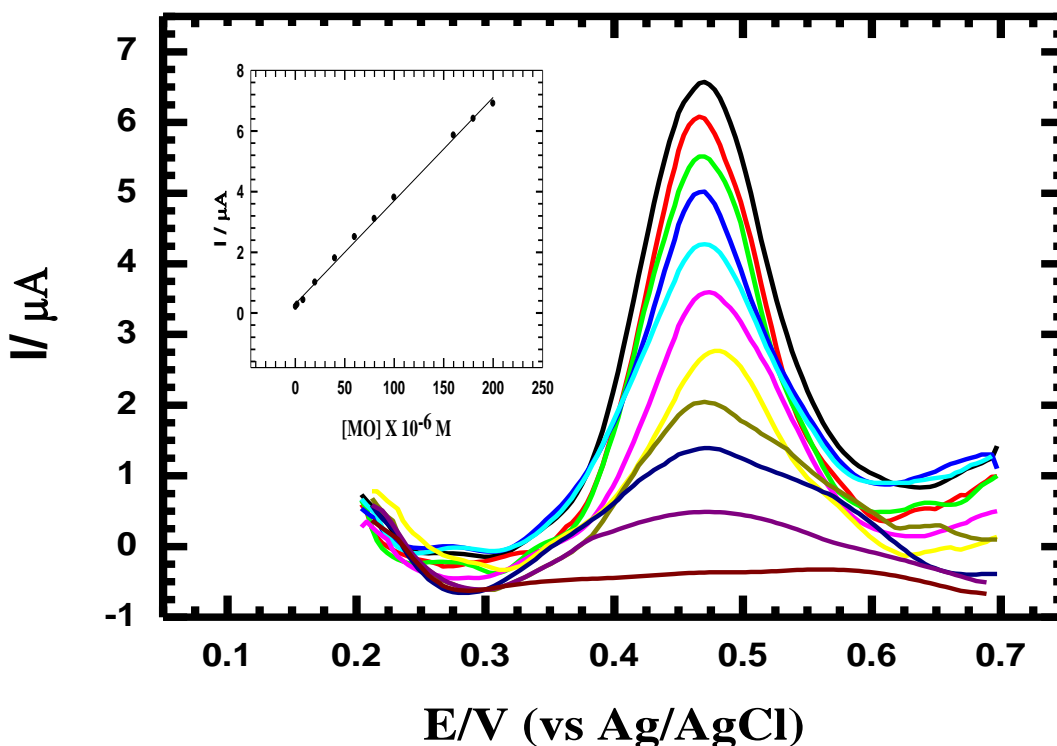


Figure 5. The effect of changing the concentration of MO, using differential pulse mode at GNMCPe in 0.04 M B-R buffer pH 7.4 and scan rate 10 mV/s. The inset: the relation between MO concentration and the current responses.

Table 2. Comparison of the GNMCPPE with the reported methods for the determination of morphine.

Electrode used	Detection limit	references
Molecularly imprinted polymer-modified electrode	0.2 mM	[22]
Cobalt hexacyanoferrate modified electrode	0.5 μ M	[24]
Pretreated GCE	0.2 μ M	[27]
Modified-palladized aluminum electrode	0.8 μ M	[31]
Ordered mesoporous carbon modified glassy carbon electrode [OMC/GCE]	50 nM	[36]
Au nanotubes arrays electrode	40 nM	[42]
GNMCPPE	4.21 nM	This work

Aliquots of the drug stock-solution (1.0×10^{-3} mol L⁻¹) were introduced into the electrolytic cell and voltammetric analyses were carried out and the voltammograms were recorded. The peak current was evaluated as the difference between each voltammogram and the background electrolyte voltammogram. All measurements were carried out at the room temperature.

Pulse voltammetric techniques such as DPV are effective and rapid electroanalytical techniques with well-established advantages, including good discrimination against background current and low detection limits.

To prove the sensitivity of the GNMCPPE towards the electrochemical measurement of MO, the effect of changing the concentration of MO in B-R buffer pH 7.4, using DPV mode is studied (Fig 5). The following are the parameters for the DPV experiments: $E_i = 200$ mV, $E_f = 700$ mV, scan rate = 10 mV.s⁻¹, pulse width = 25 ms, pulse period = 200 ms, and pulse amplitude = 10 mV. The corresponding calibration plot is given in the inset.

The calibration plot was linearly related to MO concentration over the range of 4.0×10^{-7} to 2.0×10^{-4} mol L⁻¹ with the regression equation of $I_p(\mu A) = 0.034 c(\mu M) + 0.299$ and the correlation coefficient is 0.9987.

The limit of detection (LOD) and the limit of quantitation (LOQ) are calculated from the oxidation peak currents of the linear range using the following equations:

$$\text{LOD} = 3s/m$$

$$\text{LOQ} = 10s/m$$

Where $s = 4.2 \times 10^{-4}$; is the standard deviation of the intercept (three runs) and m is the slope [μA (mol L⁻¹)⁻¹] of the related calibration curves, and they are found to be 4.21×10^{-9} mol L⁻¹ and 1.40×10^{-8} mol L⁻¹, respectively. Both LOD and LOQ values confirm the sensitivity of GNMCPPE.

Table 2 shows a comparison of the GNMCPPE with the reported methods for the determination of morphine.

3.7. Analytical application

3.7.1. Analysis of Morphine sulphate® tablets

The determination of MO in its pharmaceutical formulation (10 mg/tablet) without the necessity for any extraction steps was performed.

Five tablets of morphine sulphate are weighed and the average mass per tablet is determined, then these tablets are grinded to fine powder. A portion of the powder is dissolved to obtain 1.0×10^{-3} mol L⁻¹ solution.

Aliquots of the drug solution were introduced into the electrolytic cell and the general procedure is carried out based on the average of three replicate measurements. The average standard MO concentration is taken as a base value. Then, known quantities of morphine sulphate tablets are added to the aliquot, and its concentrations are determined following the developed procedure. The recovery and relative standard deviation are calculated and given in table 3. The results suggest that GNMCPE has high reproducibility and that there are no important matrix interferences for the samples analyzed and it would be useful electrode for quantitative analysis of MO in pharmaceutical formulations.

Table 3. Recovery data obtained by standard addition method for (MO) in drug formulation.

Formulation	[tablet] taken $\times 10^{-6}$ M	[standard] added $\times 10^{-6}$ M	Found(M) $\times 10^{-6}$ M	Recovery %	RSD %
Morphine	1.0	2.0	3.03	101.0	0.82
sulphate	8.0		10.04	100.4	0.43
	20.0		21.80	99.1	0.83
	48.0		50.32	100.6	0.59

Table 4. Evaluation of the accuracy and precision of the proposed method for the determination of (MO) in urine sample

[MO]added (M) $\times 10^{-5}$	[MO] Found ^a (M) $\times 10^{-5}$	Recovery (%)	SD $\times 10^{-6}$	S.E ^b $\times 10^{-6}$	C.L. ^c $\times 10^{-6}$
2.0	2.02	101.0	0.23	0.11	0.37
6.0	5.99	99.80	0.13	0.06	0.16
12.0	12.04	100.3	0.41	0.20	0.65
18.0	18.04	100.2	0.42	0.21	0.68

^a Mean for five determinations

^b Standard errors = SD/\sqrt{n}

^c C.L. confidence at 95% confidence level and 4 degrees of freedom ($t=2.776$)

3.7.2. Validation method in urine

Validation of the procedure for the quantitative assay of the MO in urine is examined in B-R buffer pH 7.4, at scan rate 10 mV/s using DPV. The calibration curve (fig 6) gives a straight line in the linear dynamic range $2 \times 10^{-6} \text{ mol L}^{-1}$ to $2 \times 10^{-4} \text{ mol L}^{-1}$ with correlation coefficient, $r = 0.9992$, the LOD is $8.96 \times 10^{-8} \text{ mol L}^{-1}$. Four different concentrations on the calibration curve are chosen to be repeated five times to evaluate the accuracy and precision of the proposed method which is represented in (table-4).

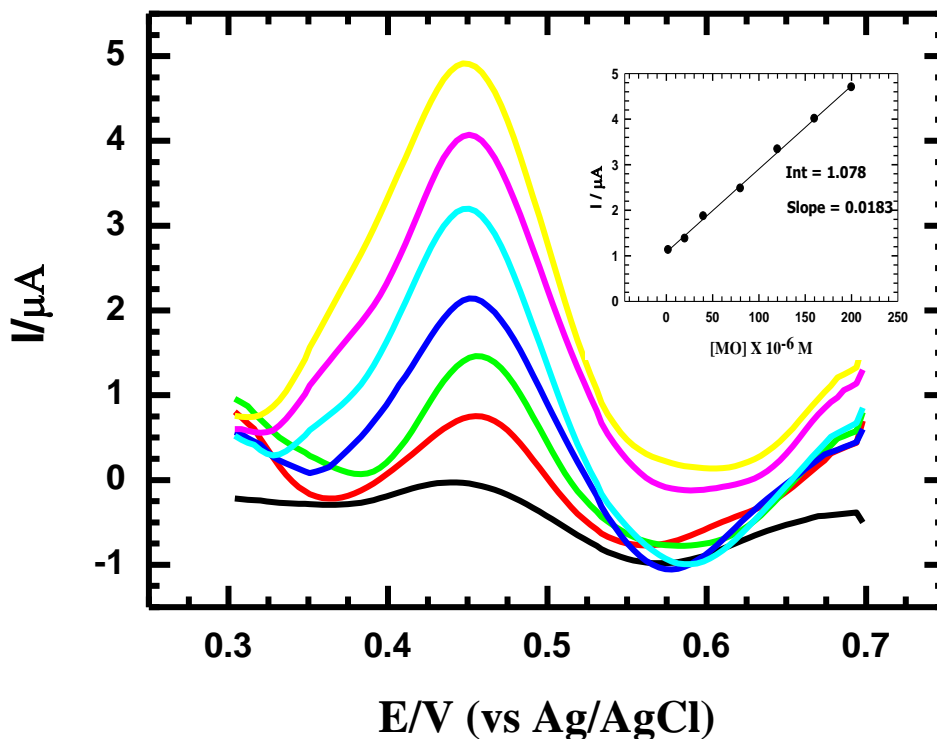


Figure 6. Validation of the quantitative assay of the MO in urine using B-R buffer pH 7.4, at scan rate 10 mV/s. The inset: the relation between MO concentration in urine and the current responses.

4. CONCLUSION

In the present work, a biosensor based on CP-electrode modified with gold nanoparticles was used for electrochemical determination of MO. The advantages of the gold nanoparticles enhanced the sensitivity of the CP-electrode significantly. The results showed that the method was simple and sensitive enough for the determination of MO in clinical preparations (human urine) and in commercial tablet under physiological conditions with good precision, accuracy, selectivity and very low detection limit (nano-molar).

ACKNOWLEDGMENT

The authors would like to express their gratitude to Cairo University (Office of Vice President for Graduate Studies and Research) for providing partial financial support through "The Young Researchers' Program." We would like to acknowledge the financial support by the National Organization for Drug Control and Research (NODCAR, Egypt).

References

1. "Morphine Sulfate". The American Society of Health-System Pharmacists. <http://www.drugs.com/monograph/morphine-sulfate.html>. Retrieved 3 April 2011.
2. T.J. Meine, M.T. Roe, A.Y. Chen, *JAHA*, 149 (6) (2005) 1043.
3. D. Schrijvers, F. Fraeyenhove, *J. Canc. Res. Ther.*, 16 (5) (2010) 514.
4. F. Naqvi, F. Cervo, S. Fields, J. Geriatr. *Psych. Neur.* 64 (8) (2009) 8.
5. M.S-Contin (Morphine) clinical pharmacology - prescription drugs and medications at Rx List.
6. W. Huang, W. Qian, P. Jain, M. El-Sayed, *Nano. Lett.*, 7 (10) (2007) 3227.
7. Om.P. Khatri, K. Murase, H. Sugimura, *Langmuir*, 24 (20) (2008) 3787.
8. L. Guzzi, G. Peto, A. Beck, K. Frey, O. Geszti, G. Molnar, C. Daroczi, *J. Am. Chem. Soc.*, 125 (14) (2003) 4332.
9. N. F. Atta, A. Galal, F. M. Abu-Attia, S. M. , *J. Electrochem. Soc.*, 157 (9) (2010) F116.
10. H. Qiu, G. Zhou, G. Ji, Y. Zhang, X. Huang, Y. Ding, *Colloid Surface B*. 69 (1) (2009) 105.
11. P.P. Rop, F. Grimaldi, J. Burle, M.N. Desaintleger, A. Viala, *Chromatogr. B*, 661(2) (1994) 245.
12. S.R. Edwards, M.T. Smith, *Chromatogr. B*, 814 (2) (2005) 241.
13. M. Mabuchi, S. Takatsuka, M. Matsuoka, K. Tagawa, *J Pharmaceut. Biomed*, 35 (3) (2004) 563.
14. J.F. Li, C. Dong , *Spectrochim. Acta A*, 71 (5) (2009) 1938.
15. K. Aoki, Y. Shilama, A. Kokado, T. Yoshida, Y. Kuroiwa, *Forensic Sc. Int.*, 81 (2-3) (1996) 125.
16. G. Sakai, K. Ogata, T. Uda, N. Miura, N. Yamazoe, *Sensor Actuat B-Chem.*, 49 (1-2) (1998) 5.
17. H. X. Hao, H. Zhou, J. Chang, J. Zhu, T. X. Wei, *Chinese Chem. Lett.*, 22(4) (2011) 477.
18. D.J. Chapman, S.P. Joel, G.W. Aherne, *J Pharmaceut. Biomed.*, 12 (3) (1994) 353.
19. P.K. Owens, L. Karlsson, E.S.M. Lutz, L.I. Anderson, *Trend. Anal. Chem.*, 18 (3) (1999) 146.
20. K. Haupt, K. Mosbach, *Chem. Rev.*, 100 (7) (2000) 2495.
21. K. C. Ho, C. Y. Chen, H. C. Hsu, L. C. Chen, S.C. Shiesh, X. Z. Lin, *Biosens. Bioelectron.*, 20 (1) (2004) 3.
22. W. M. Yeh, K.C. Ho, *Anal. Chim. Acta*, 542 (1) (2005) 76.
23. A.M. Idris, A.O. Alnajjar, *Talanta*, 77 (2) (2008) 522.
24. F. Xu, M. N. Gao, L. Wang, T. S. Zhou, L. T. Jin, J. Y. Jin JY, *Talanta*, 58 (3) (2002) 427.
25. K. C. Ho, C. Y. Chen, H. C. Hsu, L. C. Chen, S. C. Shiesh, X. Z. Lin, *Biosens. Bioelectron.*, 20 (1) (2004) 3.
26. C. H. Weng, W. M. Yeh, K. C. Ho, G. B. Lee, *Sensor Actuat B-Chem.*, 121 (2) (2007) 576.
27. F. Li, J. X. Song, D. M. Gao, Q. X. Zhang, D. X. Han, L. Niu, *Talanta*, 79 (3) (2009) 845.
28. N. F. Atta, A. Galal, R. A. Ahmed, *Electroanalysis*, 23(3) (2011) 737.
29. R.S. Schwartz, C.R. Benjamin, *Anal. Chim. Acta* 141(1982) 365.
30. B. Proksa, L. Molnár, *Analytica Chimica Acta*, 97 (1) (1978) 149.
31. H. M. Pournaghi-Azar, A. Saadatirad, *J. Electroanal. Chem.*, 624 (1-2) (2008) 293.
32. A.Niazi, A. Yazdanipour, *Chinese Chem. Lett.*, 19 (2008) 465.
33. A.Niazi, J. Ghasemi, M. Zendehtdel, *Talanta*, 74 (2) (2007) 247.
34. A.Salimi, R. Hallaj, G.R. Khayatian, *Electroanalysis*, 17 (2005) 873.
35. N. F. Atta, A. Galal, F. M. Abu-Attia, S.M. Azab, *Electrochim. Acta*, 56 (5) (2011) 2510.
36. F. Li, J. Song, C. Shana, D. Gao, X. Xua, L. Niua, *Biosens. Bioelectron.*, 25 (6) (2010) 1408.
37. X. Jiang and X. Lin, *Anal. Chim. Acta*, 537 (1-2) (2005) 145.

38. S. D. Roy, G. L. Flynn, *Pharmaceut. Res.*, 6 (2) (1989) 147.
39. N. F. Atta, S. A. Darwish, S. S. Khalil, A. Galal, *Talanta*, 72 (4) (2007) 1438.
40. W. Qijin, Y. Nianjun, Z. Haili, Z. Xinpin and X. Bin, *Talanta*, 55 (3) (2001) 459.
41. V.S. Vasantha and S.-M. Chen, *J. Electroanal. Chem.*, 592 (1) (2006) 77.
42. G. Yang, Y. Chen, L. Li, Y. Yang, *Clin. Chim. Acta*, 412 (17-18) (2011)1544.